PHYSICAL REVIEW B **80**, 241412(R) (2009)

Breakdown of the $N=0$ quantum Hall state in graphene: Two insulating regimes

L. Zhang,[1] J. Camacho,[1] H. Cao,[2] Y. P. Chen,[2] M. Khodas,[1,3] D. E. Kharzeev,[3] A. M. Tsvelik,[1] T. Valla,[1] and I. A. Zaliznyak[1,*]

[1]*CMPMSD, Brookhaven National Laboratory, Upton, New York 11973, USA*

[2]*Department of Physics, Purdue University, West Lafayette, Indiana 47907, USA*

[3]*Physics Department, Brookhaven National Laboratory, Upton, New York 11973, USA*

(Received 13 April 2009; revised manuscript received 20 November 2009; published 23 December 2009)

We studied the unusual quantum Hall effect (QHE) near the charge neutrality point in high-mobility graphene sample for magnetic fields up to 18 T. We observe breakdown of the delocalized QHE transport and strong increase in resistivities $\rho_{xx}, |\rho_{xy}|$ with decreasing Landau-level filling for $\nu<2$, where we identify two insulating regimes. First, $\rho_{xx,xy}$ increases nearly exponentially within the range of several resistance quanta R_K, while the Hall effect gradually disappears and the off-diagonal resistivity ρ_{xy} eventually becomes independent of the direction of magnetic field, consistent with the Hall insulator with local transport. Then, at a filling $\nu \approx 1/2$, there is a cusp in $\rho_{xx}(\nu)$ and an onset of even faster growth with the decreasing ν, indicating transition to a collective insulator state. A likely candidate for this state is a pinned Wigner crystal.

DOI: 10.1103/PhysRevB.80.241412 PACS number(s): 73.43.−f, 71.70.Di, 73.63.−b

Graphene is a honeycomb monolayer of C atoms, which forms the most common carbon allotrope graphite, but has only recently been isolated in the two-dimensional (2D) form.[1] A bipartite honeycomb sp^2-bonded lattice gives graphene its unique electronic structure. Two dispersion sheets associated with the electrons belonging to two different sublattices form the filled π and the empty π^* bands, which meet at two distinct isolated points (valleys K and K'), yielding pointlike Fermi surfaces. Low-energy electronic states in each valley have a linear 2D conical dispersion $\varepsilon(\mathbf{p})=v_F p$ and, in addition to 2D momentum, have a 2D pseudospin quantum number accounting for the two-sublattice structure. Such quasiparticles are formally described by the Dirac equation for chiral massless fermions and have peculiar transport properties.[2,3]

In a magnetic field H perpendicular to the graphene layer, the spectrum of Dirac quasiparticles is quantized into Landau levels (LLs) with energies $E_N=\pm\hbar\omega_c\sqrt{N}$. Plus and minus signs correspond to electrons and holes, respectively, $\omega_c=v_F\sqrt{2eH/(\hbar c)}$ is the "cyclotron frequency" for Dirac fermions, and $N=n'+1/2\pm1/2$, where $n'=0,1,2,\ldots$ enumerates orbital wave functions and $\pm1/2$ are pseudospin eigenvalues. For each E_N, there are four states, corresponding to different spin and valley indices. In the presence of Zeeman interaction and intervalley scattering, these states might split further, as illustrated in Fig. 4(d). Unlike the case of Landau quantization for nonrelativistic massive electrons, where $E_N=\hbar\omega_c(N+1/2)$ and $\omega_c=eH/(mc)$, in graphene there is a field-independent level at $E=0$ for $N=0$. At the charge neutrality point (CNP) (in undoped graphene), this level is half-filled, being equally shared between particles and holes. Experimentally, such peculiar LL structure is manifested in the unusual QHE observed in graphene,[4,5] where Hall conductivity is quantized as $\sigma_{xy}=4(l+1/2)/R_K$, l is an integer, and $R_K=h/e^2$ is the resistance quantum. The nature of electronic states on the $N=0$ level remains unclear and has recently become the focus of considerable attention.[3,6–10]

Here we report an experimental investigation of charge transport in a high-mobility graphene sample for low carrier density n near the CNP and in magnetic fields up to 18 T, that is, in the QHE regime near the $N=0$ Landau level, where previous studies have yielded conflicting results.[6–10] In particular, some studies have found finite longitudinal resistance $\rho_{xx}\sim R_K$ near the CNP even for high magnetic fields, where the plateau at $\rho_{xy}=R_K/2$ around $\nu=n\Phi_0/H=\pm2$ (Φ_0 is the flux quantum) corresponding to either particle or hole filling of the two lowest $N=0$ LL is well developed.[6–8] Others, reported $\rho_{xx}\gg R_K$, in the MΩ range, indicating an insulating $N=0$ state at high fields.[9,10] In Ref. 10, the $\rho_{xx}(H)$ divergence with H was analyzed as an *ad hoc* Kosterlitz-Thouless transition and associated with a critical field H_c (rather than a filling ν_c), which was found to be sample dependent. The discrepancies between different measurements could be somewhat reconciled by the fact that cleaner samples show stronger divergence of $\rho_{xx}(H)$ with increasing H in the $N=0$ state.[10] Hence, sample quality appears crucial for understanding the physics of the $N=0$ LL state in graphene.

We have studied a monolayer graphene sample prepared by mechanical exfoliation of ZYA grade highly oriented pyrolytic graphite on a Si/SiO_2 substrate using the standard procedure described in Ref. 1. Transport properties summarized in Figs. 1(a) and 1(b) reveal high quality of our sample. Magnetoresistance measurements were performed using the low-frequency (17.777 Hz) lock-in technique with a driving current $I=10$ nA and the 18 T superconducting magnet at the National High Magnetic Field Laboratory (NHMFL). The follow-up measurements in fields up to 6 T were performed at Purdue University. The sample mobility between the two measurements remained unchanged within the error $\mu=2.82(6)\times10^4$ cm^2/V/s, while the CNP has shifted by ≈2 V. At $T=150$ K, μ decreased by less than 10%, to $\mu(150K)\approx2.6\times10^4$ cm^2/V/s. A slight electron-hole asymmetry of the resistance in Fig. 1 is typical of devices with invasive contacts [see inset in Fig. 1(b)] and is explained by the work-function difference between graphene and the Au/Cr electrodes in our device.[12]

Figure 2 summarizes the QHE in our sample for three charge-carrier densities near the CNP, $n=1\times10^{11}$, 3.2

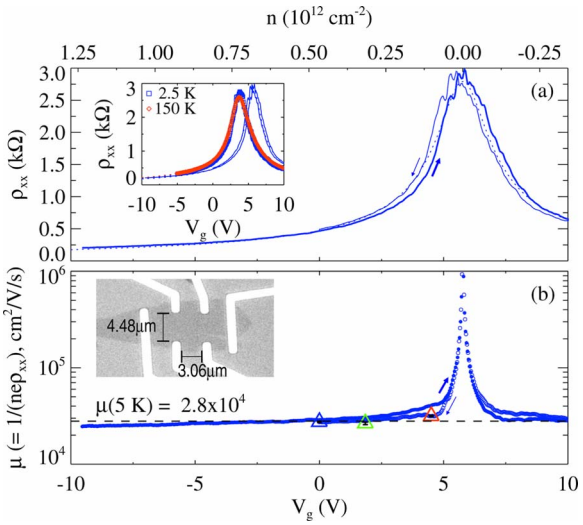

FIG. 1. (Color online) Longitudinal resistivity ρ_{xx} of our sample in zero magnetic field as a function of the gate voltage V_g. (a) Solid lines are ρ_{xx} at $T=5$ K for increasing (thick) and decreasing (thin) V_g, as indicated by arrows. Small hysteresis results from mobile charges in Si/SiO_2 substrate. The inset shows the same data together with the results of similar follow-up measurements at $T=2.5$ K and $T=150$ K. Dotted lines are fits to $\rho_{xx}=1/\sqrt{\sigma_{\min}^2+(e\mu n)^2}$. (b) Drude mobility $\mu=1/(ne\rho_{xx})$ (Ref. 11). The dashed line shows $\mu=2.82(6)\times10^4$ $cm^2/V/s$, resulting from the fit. Filled and open symbols correspond to different V_g sweep directions shown by arrows. Triangles are Hall mobilities obtained from fits to the data in Fig. 2(d). The inset is the optical image of our sample.

$\times10^{11}$, and 4.7×10^{11} cm^{-2}. The latter was refined by fitting the low-field linear part of the Hall resistivity to $\rho_{xy}(H)=H/(nec)$ [Fig. 2(a)]. This yields $dn/dV_g=-8.07(9)\times10^{10}$ cm^{-2}/V. Clear plateaux corresponding to half the resistance quantum in ρ_{xy} and zero ρ_{xx} develop for all three carrier densities upon approaching the LL filling $|\nu|=2$ [Figs. 2(a)–2(c)]. This is a hallmark of the QHE in graphene, resulting from only two of the total four $N=0$ LL being available to either electrons or holes [Fig. 4(d)]. Hence, two conducting channels and $\rho_{xy}=\pm R_K/2$ plateaux. The developed QHE regime is also manifested by the plateau at $\pi/2$ in the Hall angle $\theta_{\rm Hall}=\arctan(\rho_{xy}/\rho_{xx})$ [Fig. 2(d)]. Fitting the low-field linear part of $\theta_{\rm Hall}$ to the result of the Boltzman transport theory, $\tan(\theta_{\rm Hall})=(\mu/c)H$, allows for an alternative refinement of the sample mobility μ [dash-dotted lines in Fig. 2(d)]. The obtained Hall mobility agrees very well with the Drude field mobility [Fig. 1(b)].

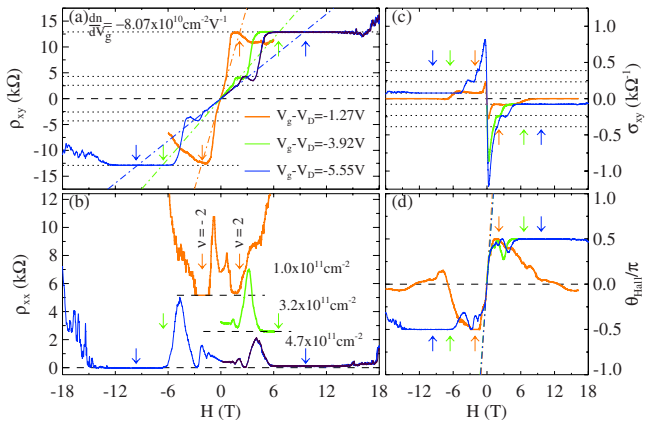

FIG. 2. (Color online) QHE in our sample for different gate offsets V_g-V_D from the Dirac point V_D, i. e. for different carrier densities n. (a) ρ_{xy}, (b) ρ_{xx}, (c) σ_{xy}, and (d) Hall angle $\theta_{\rm Hall}$. $\nu=\pm2$ filling for each n is shown by the corresponding arrow. Dash-dotted lines in (a) are linear fits of the low-field part of $\rho_{xy}(H)$ used to refine the Hall constant and obtain $n=H/[ec\rho_{xy}(H)]$. Curves in (b) are shifted for clarity; the zero level for each is given by the broken horizontal line. Horizontal dotted lines in (a) and (c) show the resistance and the conductivity quantization in graphene.

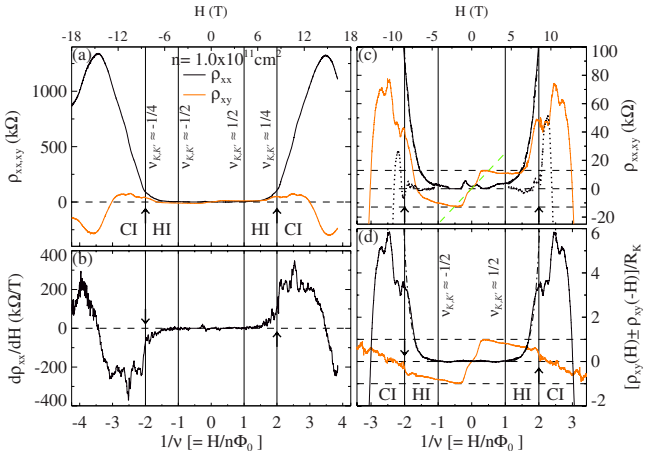

FIG. 3. (Color online) Breakdown of QHE in graphene for $n\approx10^{11}$ cm^{-2} and $T=0.25$ K. Top scale shows magnetic field H corresponding to the inverse LL filling $1/\nu$ on the bottom. Filling per valley is $\nu_{K,K'}\approx\nu/2$. (a) $\rho_{xx}(H)$ (dark) and $\rho_{xy}(H)$ (light); (b) $d\rho_{xx}(H)/dH$. Dramatic increase in $\rho_{xx}(H)$ beyond a cusp at $\approx4R_K$ and a steplike anomaly in $d\rho_{xx}(H)/dH$ indicate transition to a collective insulator state at $\nu\approx\pm1/2$. (c) Blowup of the initial growth in $\rho_{xx,xy}(H)$ and (d) the sum (dark) and the difference (light) of ρ_{xy} for two opposite directions of magnetic field show the disappearance of the Hall component following the breakdown of $|\nu|=2$ QHE state with increasing H [see also Figs. 2(a) and 2(b)]. Dash-dotted curves in (c), (d) nearly coincident with the data in the HI phase at $1\gtrsim|\nu|\gtrsim1/2$ are fits to an exponential increase $\rho_a(H)=ae^{b(|H|-H_c)}$ (Ref. 15). Dotted curve in (c) is the difference $\rho_{xx}(H)-\rho_a(H)$.

When LL filling decreases far enough past $|\nu|=2$ with the increasing magnetic field, the QHE resistance quantization breaks down and the system enters a resistive state, where $\rho_{xx}(H)>0$ and fluctuates widely with H. This fluctuating behavior of $\rho_{xx}(H)$ and $\rho_{xy}(H)$ in Figs. 2(a) and 2(b) is reproducible. In fact, the $H>0$ parts of the curves for $n=4.7\times10^{11}$ cm^{-2} overlay results of three different field sweep measurements, which essentially coincide. While for this carrier density LL filling in our field range is $\nu\gtrsim1$ and $\rho_{xx,xy}(H)$ increase only moderately, much lower $N=0$ LL fillings $\nu\ll1$ are achievable for $n=10^{11}$ cm^{-2}. Here, we observe a dramatic increase in $\rho_{xx,xy}(H)$, which is detailed in Fig. 3. In terms of the Hall conductivity, it appears as a "zero plateau" state with $\sigma_{xy}=0$ around $\nu=0$ [Fig. 2(c)]. However, the magnetic field reversal (Onsager) symmetry $\rho_{xy}(H)=-\rho_{xy}(-H)$ is violated in this state, indicating a breakdown of the dissipationless QHE transport via delocalized states, typical of a

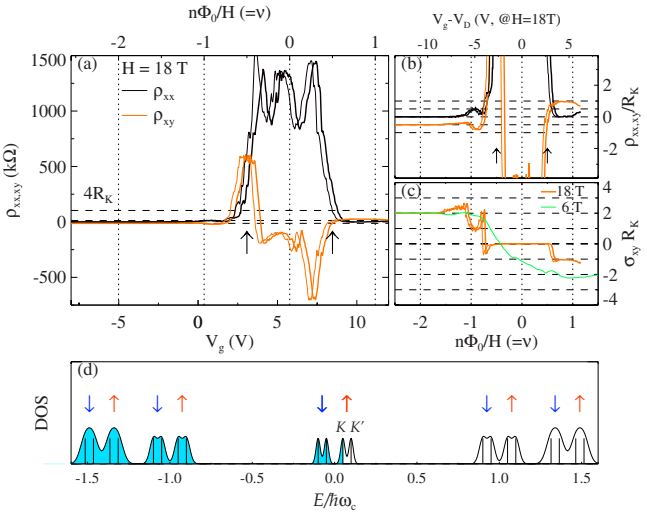

FIG. 4. (Color online) Breakdown of the quantum Hall state in graphene at $H=18$ T as a function of gate voltage (carrier concentration) at $T=0.25$ K. (a) Onset of a strong increase in ρ_{xx} and $|\rho_{xy}|$ beyond $\approx 4R_K$ near filling $\nu=\pm 1/2$ (shown by arrows). Blowup of ρ_{xy} in (b) and σ_{xy} in (c) show a well-developed QHE plateau around $\nu=-2$ and a hint of plateaux developing at $|\nu|=1$ at R_K and $1/R_K$, respectively. The apparent $\nu=0$ plateau in (c) corresponds to a bulk insulator with zero Hall angle and no Hall effect. (d) Schematics of Landau levels in graphene, including Zeeman splitting (up/down arrows) and K,K' valley splitting (bars).

Hall insulator (HI).[13] This behavior is further emphasized by the Hall angle dependence in Fig. 2(d), which deviates from the $|\theta_{\mathrm{Hall}}(H)|=\pi/2$ QHE plateau and tends toward zero in high magnetic field.

The breakdown of the Hall effect and the development of an insulating state induced by magnetic field in our sample for $n=10^{11}$ cm^{-2} are further quantified in Fig. 3. Panel (a) shows the full range of $\rho_{xx}(H)$ and $\rho_{xy}(H)$ variation, whose initial parts are also included in Fig. 2. Careful examination of the data allows identifying distinct transport regimes. First, for some ν in the range $1\lesssim\nu\lesssim 2$, the QHE resistance quantization breaks down and a resistive state forms. The Hall angle becomes $|\theta_{\mathrm{Hall}}|<\pi/2$, but $\rho_{xy}(H)=-\rho_{xy}(-H)$ relation still holds, as shown by the sum of Hall resistivities for two opposite magnetic field directions $\rho_{xy}(H)+\rho_{xy}(-H)\approx 0$ in Fig. 3(d). Such behavior could be a sign of the full splitting of $N=0$ level shown in Fig. 4(d) and of a developing $\nu=1$ plateau or of the unusual resistive Hall metal state at $N=0$ LL considered in Refs. 6 and 14.

In the $1/2\lesssim\nu\lesssim 1$ regime, the Hall effect gradually disappears. A field-symmetric component breaking the magnetic field reversal symmetry appears in the transverse resistivity ρ_{xy}, such that $\rho_{xy}(H)\neq-\rho_{xy}(-H)$. The antisymmetric Hall component $\rho_{xy}(H)-\rho_{xy}(-H)$ decreases, while $\rho_{xx}(H)$ and $\rho_{xy}(H)$ steadily increase, reaching several resistance quanta $\lesssim 4R_K$. Both $\rho_{xx}(H)$ and the symmetrized $\rho_{xy}(H)+\rho_{xy}(-H)$ follow the same exponential dependence $\rho_a(H)=ae^{b(|H|-H_c)}$ shown by dash-dotted lines in Figs. 4(c) and 4(d). Independent fits in panels (c) and (d) give consistent $H_c=4.6(2)$ T, corresponding to $\nu\approx 1$, or a filling $\nu_{K,K'}\approx\nu/2\approx 0.5$ per valley.

Such behavior can be understood as a HI (Refs. 6 and 13), resulting from the Zeeman splitting of the $N=0$ LL [Fig. 4(d)]. In this case, the delocalized quantum Hall state and the related $N=0$ mobility edge shift to a finite energy $E_0\approx g\mu_B H$ (g is the Lande factor and μ_B is the Bohr's magneton). For filling factors below $\nu\approx 1$, the chemical potential falls below E_0 and the electrons are localized. Thermally activated Hall transport via delocalized states is possible for $T>0$, but it vanishes with the increasing field-induced spin splitting of the $N=0$ level. At $T\approx 0$, the system is insulating, the transport occurs via hopping between localized states, and is dominated by the mesoscopic conductance fluctuations in the sample. The transverse voltage drop results from the sample and the leads average asymmetry. The $I-V$ curve is expected to be strongly nonlinear, as it was indeed observed in Ref. 10, although authors there have interpreted this nonlinearity as resulting from sample heating. A similar $N=0$ insulating regime in a lower mobility sample was recently reported in Ref. 15.

Probably the most surprising and intriguing is the $\nu\lesssim 1/2$ regime, which is characterized by marked changes in behavior of $\rho_{xx}(H)$ and $\rho_{xy}(H)$. Both $\rho_{xx}(H)$ and the symmetrized $\rho_{xy}(H)+\rho_{xy}(-H)$ deviate from the exponential growth describing the HI phase. The deviation from the fit $\rho_{xx}(H)-\rho_a(H)$ is shown by the dotted line in Fig. 3(c). It emphasizes cusp in $\rho_{xx}(H)$, which is also visible in Fig. 3(a), and which is followed by an abrupt increase in resistance beyond $\rho_{xx}\sim 4R_K$. The cusplike singularity in $\rho_{xx}(H)$ is also identified by the prominent jump in the derivative $d\rho_{xx}/dH$ at $\nu\approx 1/2$ [Fig. 3(b)]. The Hall component of the transverse resistivity given by the difference $\rho_{xy}(H)-\rho_{xy}(-H)$ also shows singular behavior, abruptly approaching zero at the same filling [Fig. 3(d)], so that $\rho_{xy}(H)\approx\rho_{xy}(-H)$ for $\nu\lesssim 1/2$.

Simultaneous singular behavior of $\rho_{xy}(H)-\rho_{xy}(-H)$ and $d\rho_{xx}/dH$ at $\nu\approx 1/2$ indicate transition to a different, more insulating state, which we identify as a collective insulator (CI). A likely candidate for such a CI state is a pinned Wigner crystal (WC), where electrons are collectively rather than individually localized. Our interpretation is based upon the analogy with QHE in high-mobility 2D electron gases (2DEG) in semiconductor heterostructures, where an onset of strongly insulating behavior at low filling factors $\nu\lesssim 1/4$ has also been reported.[16–18] In 2DEG, this CI behavior is understood as a 2D WC, which can be pinned by an arbitrarily small disorder at $T=0$ K.[19,20] In our case of graphene, transition at $\nu\approx 1/2$ corresponds to a filling $\nu_{K,K'}\approx 1/4$ per valley, roughly consistent with 2DEG results.

Finally, we have also investigated the breakdown of the $N=0$ quantum Hall state and the appearance of the insulating behavior in our graphene sample by varying the gate voltage V_g in magnetic field $H=18$ T. The results shown in Fig. 4 are in agreement with those in Fig. 3, corroborating the picture presented above. There is a well-developed QHE plateau around filling $|\nu|=2$. The quantization breaks down in the $1\lesssim|\nu|\lesssim 2$ range and there is a hint of a plateau at $|\rho_{xy}|=R_K$ developing around $|\nu|\approx 1$ [Figs. 4(b) and 4(c)]. An onset of strong increase in ρ_{xx} and $|\rho_{xy}|$ beyond $\sim 4R_K$ is seen at $|\nu|\approx 1/2$. It can also be traced in the behavior of the derivative $d\rho_{xy}/dV_g$. The fact that such an abrupt onset occurs here and in Fig. 3 at very different $|n|$ and $|B|$ but similar $|\nu|$

$=|nh/eH| \approx 1/2$ suggests that it is driven by the interaction between electrons in graphene, again consistent with a transition to a bulk collective insulator at $|\nu| \lesssim 1/2$. Due to the contact-induced electron-hole asymmetry, there is a slight shift of the curves in Fig. 4 with respect to the nominal $n=0$, making such measurements by sweeping V_g less favorable compared to the sweep of magnetic field at a constant V_g.

In summary, we have investigated the breakdown of the quantum Hall effect and the emergence of an insulating behavior in the $N=0$ Landau Level in a high-mobility single-layer graphene sample. The LL filling in the range $|\nu| \lesssim 2$ is achieved by either increasing the magnetic field at a constant carrier density n or by varying $n(V_g)$ at $H=18$ T. Careful analysis of our data leads us to identify two different insulating regimes as a function of the decreasing LL filling $\nu = n\Phi_0/H$. First, the well-developed resistance quantization on the $|\nu|=2$ plateau breaks down and a dissipative state develops near the LL filling $|\nu| \approx 1$. This can be understood as a HI resulting from the Zeeman splitting of the $N=0$ level, similar to that observed for higher N states.[7,9,15] For $N=0$, however, there remain no delocalized states occupied by electrons (holes) at sufficiently low filling $|\nu| \lesssim 1$, as a result of this splitting [Fig. 4(d)], and the transport is local at $T \to 0$. This observation agrees with recent findings reported in Ref. 15 and largely rules out the picture of a Hall metal with spin-polarized chiral currents,[6] although not its refined version in Ref. 14, which effectively leads to a HI.

Our most striking finding, though, is a well-defined onset of the marked resistance increase with decreasing filling at $\nu \approx 1/2$. It is clearly revealed by the anomalies in the field dependencies $\rho_{xx}(H)$ and $\rho_{xy}(H)$ and can be understood as a transition from the local HI to a bulk collective insulator state. Collective bulk insulating states have been previously observed in 2DEG systems at low filling ν and are commonly associated with pinned Wigner crystals.[16–20] We suggest that a pinned WC is also a likely candidate for the strongly insulating state, which we have identified in our graphene sample for $|\nu| \lesssim 1/2$.

We thank I. Childres, J.-H. Park, and E. Palm for help with the measurements and S. Suchalkin, Z. Jiang, M. Strongin, D. Abanin, and A. Shytov for discussions. We also thank F. Camino, A. Stein, and D. Nykypanchuk for help at the Brookhaven Center for Functional Nanomaterials, where our samples were prepared. This work was supported by the U.S. DOE under the Contract No. DE-AC02-98CH10886. Partial support by Purdue University and Miller Family Endowment is gratefully acknowledged. Work at the NHMFL is also supported by the NSF through Grant No. DMR-0084173 and by the State of Florida.

*Corresponding author; zaliznyak@bnl.gov

[1] K. S. Novoselov, A. K. Geim, S. V. Morozov, D. Jiang, Y. Zhang, S. V. Dubonos, I. V. Grigorieva, and A. A. Firsov, Science **306**, 666 (2004).
[2] C. W. J. Beenakker, Rev. Mod. Phys. **80**, 1337 (2008).
[3] A. H. Castro Neto, F. Guinea, N. M. Peres, K. S. Novoselov, and A. K. Geim, Rev. Mod. Phys. **81**, 109 (2009).
[4] K. S. Novoselov, A. K. Geim, S. V. Morozov, D. Jiang, M. I. Katsnelson, I. V. Grigorieva, S. V. Dubonos, and A. A. Firsov, Nature (London) **438**, 197 (2005).
[5] Y. Zhang, Y. W. Tan, H. L. Stormer, and P. Kim, Nature (London) **438**, 201 (2005).
[6] D. A. Abanin, K. S. Novoselov, U. Zeitler, P. A. Lee, A. K. Geim, and L. S. Levitov, Phys. Rev. Lett. **98**, 196806 (2007).
[7] A. J. M. Giesbers, U. Zeitler, M. I. Katsnelson, L. A. Ponomarenko, T. M. Mohiuddin, and J. C. Maan, Phys. Rev. Lett. **99**, 206803 (2007).
[8] Z. Jiang, Y. Zhang, H. L. Stormer, and P. Kim, Phys. Rev. Lett. **99**, 106802 (2007).
[9] Y. Zhang, Z. Jiang, J. P. Small, M. S. Purewal, Y.-W. Tan, M. Fazlollahi, J. D. Chudow, J. A. Jaszczak, H. L. Stormer, and P. Kim, Phys. Rev. Lett. **96**, 136806 (2006).
[10] J. G. Checkelsky, L. Li, and N. P. Ong, Phys. Rev. Lett. **100**, 206801 (2008); Phys. Rev. B **79**, 115434 (2009).
[11] Y.-W. Tan, Y. Zhang, K. Bolotin, Y. Zhao, S. Adam, E. H. Hwang, S. Das Sarma, H. L. Stormer, and P. Kim, Phys. Rev. Lett. **99**, 246803 (2007).
[12] B. Huard, N. Stander, J. A. Sulpizio, and D. Goldhaber-Gordon, Phys. Rev. B **78**, 121402(R) (2008).
[13] M. Hilke, D. Shahar, S. H. Song, D. C. Tsui, Y. H. Xie, and D. Monroe, Nature (London) **395**, 675 (1998).
[14] E. Shimshoni, H. A. Fertig, and G. V. Pai, Phys. Rev. Lett. **102**, 206408 (2009).
[15] A. J. M. Giesbers, L. A. Ponomarenko, K. S. Novoselov, A. K. Geim, M. I. Katsnelson, J. C. Maan, and U. Zeitler, Phys. Rev. B **80**, 201403(R) (2009).
[16] H. W. Jiang, R. L. Willett, H. L. Stormer, D. C. Tsui, L. N. Pfeiffer, and K. W. West, Phys. Rev. Lett. **65**, 633 (1990).
[17] S. D. Suchalkin, Yu. B. Vasil'ev, M. Zundel, G. Nachtwei, K. von Klitzing, and K. Eberl, JETP Lett. **74**, 564 (2001).
[18] Y. P. Chen, G. Sambandamurthy, Z. H. Wang, R. M. Lewis, L. W. Engel, D. C. Tsui, P. D. Ye, L. N. Pfeiffer, and K. W. West, Nat. Phys. **2**, 452 (2006).
[19] U. Merkt, Phys. Rev. Lett. **76**, 1134 (1996).
[20] H. A. Fertig, Phys. Rev. B **59**, 2120 (1999).